



Green Synthesis and Multifunctional Characterization of *Capparis decidua*-Mediated Iron Oxide Nanoparticles for Enhanced Antioxidant and Therapeutic Applications

Abdul Majeed Ansari¹, Dr. Dinesh Kullhary²

¹Research Scholar, School of Basic & Applied Sciences, Career Point University, Kota (Raj.)

²Research Supervisor, School of Basic & Applied Sciences, Career Point University, Kota (Raj.)

¹Email: amansaricpu@gmail.com

Abstract

The growing need of biocompatible nanomaterials that possess therapeutic activity has put the paradigm of green synthesis in the centre-stage of nanotechnological research. This study documents the synthesis of iron oxide nanoparticles (FeNPs) through a phytochemical-mediated synthesis using aqueous leaf extracts of xerophytic shrub *Capparis decidua* which is a natural source of bioactive polyphenols, alkaloids and flavonoids. Under controlled thermal conditions (60 -70 °C) the synthesis used ferric chloride hexahydrate as the metallic precursor to give spherical nanoparticles whose hydrodynamic diameter is 88.5nm (DLS) and core size is 48-87nm (SEM). The FTIR-based comprehensive characterization revealed the existence of the phenolic hydroxyl group (3403 cm⁻¹), amide groups (1643, 1541 cm⁻¹) and FeO stretching bands (664 cm⁻¹), which verified the existence of the phytochemical-mediated reduction and stabilization processes. The electrostatic repulsion of zeta potential -28.3mV exhibited strong colloidal stability. Multifunctional antioxidant analysis showed outstanding radical scavenging capacities against the DPPH (IC₅₀: 47.82±1.86 µg/mL) and the ABTS (IC₅₀: 64.31 0.97 1 -1 mL) radicals and nitric oxide radicals (IC₅₀: 68.54±0.79 µg/mL) which was close to the ascorbic acid standards. This combination of sustainable synthesis protocols and strong bioactivities makes the FeNPs one of the promising candidates in therapeutic use in oxidative stress management, nanomedicine and biomedical interventions.

Keywords: Green nanotechnology, *Capparis decidua*, Iron oxide nanoparticles, Phytochemical reduction, Antioxidant activity, Radical scavenging



1. Introduction

The latest paradigm shift in favor of environmentally benign nanotechnology has intensively triggered the studies of plant-mediated synthesis of metallic nanoparticles to provide sustainable alternatives to traditional chemical and physical synthesis methods that use dangerous reagents and energy-intensive procedures (Singh et al., 2023; Chakraborty et al., 2022). Green synthesis takes advantage of reducing, stabilising properties of phytochemicals such as polyphenols, flavonoids, alkaloids and terpenoids to promote nanoparticle nucleation and growth at ambient conditions or at slightly higher temperature (Ovais et al., 2018). This biological method gets rid of toxic reducing agents like sodium borohydride or hydroxylamine's and at the same time transfers biocompatibility and inherent therapeutic characteristics to the produced nanomaterials by forming a biomolecular corona (Shaikh et al., 2021). Magnetite (Fe_3O_4) and maghemite ($\gamma\text{-Fe}_2\text{O}_3$) types of iron oxide nanoparticles have received a considerable amount of interest in biomedical studies because of their superparamagnetic nature, biocompatibility, and versatile ability to be functionalized to accomplish a wide range of applications, including targeted drug delivery, magnetic resonance imaging contrast enhancement, hyperthermia therapy, and biosensing (Kumar et al., 2021; Parveen et al., 2018). The combination of the concepts of green synthesis and the nanotechnology of iron oxide led to nanomaterials with synergistic therapeutic effects as a result of the inorganic core and the capping agents (made of phytochemicals) (Das et al., 2020).

Capparis decidua (Forsskal) Edgew., also called karira or desert caper, is an underutilised botanical resource in nanotechnological research, even though it has been reported to be rich in phytochemicals, and also has a long-standing history of traditional medical use. It is an xerophytic shrub that grows in arid areas of South Asia and Middle East environments and undergoes harsh environmental conditions as an adaptive strategy (Singh et al., 2011). Past phytochemical studies have found that *C. decidua* is rich in bioactive constituents such as glucosinolates (glucocapparin, glucoiberin), alkaloids (stachydrine, capparine, decidarine), flavonoid glycosides (rutin, quercetin, kaempferol), phenolic acids (gallic, chlorogenic, caffeic acids), phytosterols (2-sitosterol, stigmasterol), and essential fatty acids. These compounds are multifunctional biologically active with antioxidant, anti-inflammatory, antimicrobial, and hypoglycaemic activity, which makes *C. decidua* an attractive source of



phytochemicals to produce functional nanomaterials. It has been widely reported that the phenolic compounds play a mechanistic role in nanoparticle bioreduction through the process of electron donation by electron-rich hydroxyl moieties to metallic ions, leading to their reduction to zero-valent or oxide states (Amini & Akbari, 2019; Salgado et al., 2019). At the same time, macromolecular constituents, such as proteins, polysaccharides, and others, adsorb onto the surfaces of nascent nanoparticles, which stabilises them against aggregation through steric and electrostatic forces (Pradeep et al., 2021). This two-fold activity of plant extracts eliminates the need to use external reducing and capping reagents, making the production process cost-effective and safe to the environment.

Although the current literature on phyto-based generation of iron oxide nanoparticles is growing, a clear gap in the literature is the lack of systematic studies using *C. decidua* extracts. In addition, multifunctional characterisation combining physicochemical properties and biological functions must be extensively employed in order to scale-up laboratory-scale syntheses to potential therapeutic usage. The current study fills this research gap by documenting the green synthesis of green synthesised FeNPs using *C. decidua* with systematic characterisation of morphological, spectroscopic, and colloidal properties with a complemented characterisation of multifaceted antioxidant activities using complementary radical scavenging assays. The general aim is to develop a reproducible, scaleable synthesis of biocompatible FeNPs with therapeutically useful antioxidant activities to be used in the future in the field of oxidative-stress amelioration and nanomedicine.

2. Materials and Methods

2.1 Plant Material Collection and Extract Preparation

Fresh wild *Capparis decidua* was collected and washed thoroughly with running tap water to remove the surface contaminants and the particles. The filtered plant material (10g) was macerated in small pieces, and blended in 100mL of ultrapure double-distilled water keeping the ratio of biomass and solvent at 1:10 (w/v). The suspension was heated to 100°C on a hot plate and then intermittently swirled at specific intervals in 15-20 minutes to extract thermostable phytochemicals. After thermal extraction, the decoction was cooled to room temperature and vacuum filtered using Whatman No.1 filter paper (pore size: 11 µm) in order to get a clear extract. The filtrate was kept at 4°C temperature in amber glass containers to



reduce photodegradation and oxidative degradation of labile phytoconstituents until further use.

2.2 Green synthesis of Iron Oxide Nanoparticles

The bioreduction synthesis was done with ferric chloride hexahydrate ($\text{FeCl}_3 \cdot 6\text{H}_2\text{O}$, >99% purity, Sigma-Aldrich) as the source of iron. $\text{FeCl}_3 \cdot 6\text{H}_2\text{O}$ solution (0.1M) was dropwise added to 100 mL of the freshly prepared *C. decidua* extract heated on a magnetic stirrer at temperature between 60 and 70°C and continuous swirling at 300 rpm. The colour change of the reaction mixture gradually between pale yellow-green to dark brown and finally to black was used as a visual indicator of formation of nanoparticles. The mixture was stirred 2–3h to achieve maximum reduction and sufficient time to ensure that the nanoparticles were nucleated, grew, and stabilised by phytochemicals. The resulting colloidal suspension was left to cool at room temperature and then centrifuged at 10000 rpm for 20 minutes. The precipitated FeNPs were washed three times with the ultrapure water and absolute ethanol and dried in oven at 60°C overnight. The collected nanoparticles were dried, fine powder was obtained using mortar and pestle and stored in desiccated conditions to be characterised and subsequently used in bioassays.

2.3 Physicochemical Characterization.

2.3.1 UV-Visible Spectroscopy : The aliquots of the colloidal suspension were diluted and scanned through the wavelength range of 200-700nm with a resolution of 1nm to identify typical surface plasmon resonance peaks and electronic transitions related to interaction of iron oxide nanoparticles.

2.3.2 Fourier Transform Infrared Spectroscopy (FTIR): The FeNP powder samples were dried and pelleted in KBr. The spectra were measured in the mid-infrared ($4000\text{-}400\text{ cm}^{-1}$) with a spectral resolution of 4 cm^{-1} in a total of 32 summative scans to improve signal-to-noise ratio. To reduce the interference caused by ambient water vapour and carbon dioxide, baseline correction and atmospheric compensation were used.

2.3.3. Scanning Electron Microscopy (SEM): Field-emission scanning electron microscopy (FE-SEM, JEOL JSM-7600F) with an accelerating voltage of 10-20kV was used to perform morphological analysis and size distribution analysis. The dried FeNPs was dispersed in



absolute ethanol by ultrasonication. The suspension was drop-casted over silicon wafer substrate and let dry. Samples were sputter-coated with thin layer of gold (about 5-10nm) before imaging to increase the electrical conductivity of the sample and eliminating charging artefacts.

2.3.4 Dynamic Light Scattering (DLS) and Zeta Potential: Zeta potential, polydispersity index (PDI) and hydrodynamic diameter values were obtained using a Malvern Zetasizer Nano ZS with a helium neon laser at 633 nm and combined with a back-scatter detector at 173°C. FeNPs (0.1·mg/mL) were suspended in ultrapure water and subjected to ultrasonication in order to break aggregates. Measures were done three times (at 25°C) and every run consisted of at least 12 sub-runs to establish statistical reliability. Electrophoretic mobility was used to calculate the zeta potential which was then followed up by using the Smoluchowski equation.

2.4.1 Antioxidant activity Assays.

2.4.1 DPPH Radical Scavenging Assay

The free radical scavenging ability was evaluated against stable 1,1-diphenyl-2-picrylhydrazyl (DPPH) radical. A stock solution of FeNP at concentration level of 20 to 100 µg/mL in ultra clean water was prepared. DPPH solution (0.1 mM) was made in absolute methanol. The solution mixture of FeNP solution (1mL) and DPPH solution (3mL) was incubated in the dark at room temperature for 30 minutes. A UV-Visible spectrophotometer was used to measure absorbance at the wavelength of 517nm with a methanol blank. Ascorbic acid was used as the positive control. The percent inhibition was determined by the following equation:

$$\% \text{ Inhibition} = \frac{[\text{Abs. control} - \text{Abs. sample}]}{\text{Abs. control}} * 100$$

The non-linear regression analysis was done to determine the IC₅₀ value.

2.4.2 ABTS Radical Cation Scavenging Assay

The ABTS⁺ radical cation decolorization test was conducted to analyse electron transfer. ABTS radical was formed by reacting 7mM 2,2-azino-bis(3-ethylbenzothiazoline-6-sulfonic acid diammonium salt with 2.45mM potassium persulfate in equal volume and incubation in



darkness at room temperature. The resulting dark-green ABTS⁺ solution was then diluted using phosphate-buffered saline (PBS, pH 7.4) to achieve an absorbance of 0.70 ± 0.02 at 734nm. The 20-100 $\mu\text{g/mL}$ solutions of FeNP were mixed with 3 mL of the diluted ABTS⁺ and allowed to react for upto 6 min at room temperature, then the absorbance was recorded at 734 nm. The values of percent inhibition and IC₅₀ were obtained by using the equation:

$$\% \text{ Inhibition} = \frac{[Abs. control - Abs. sample]}{Abs. control} * 100$$

The non-linear regression analysis was done to determine the IC₅₀ value.

2.4.3 Nitric Oxide Radical Scavenging Assay

Nitric-oxide radical scavenging activity was analyzed using sodium nitroprusside (SNP) as an NO donor. A solution of SNP (10mM) in phosphate buffer (pH 7.4) was added to different concentrations of FeNP solution (20-100 $\mu\text{g/mL}$) in a 1:1 volume ratio. The mixture that was incubated at 25°C in the presence of light for 150 min to allow the generation of photolytic NO. After incubation, 500 μL of the reaction mixture was combined with 500 μL of Griess reagent and incubated for 10 minutes. The absorbance at 546nm was measured and percent inhibition was established as compared to control Ascorbic acid.

2.5 Statistical Analysis

Each experiment was performed in triplicate and the values were represented as mean \pm SD. GraphPad Prism was used to calculate non-linear regression analysis for IC₅₀ values.

3. Results and Discussion

3.1. Phytochemical-Mediated Synthesis and Optical Characterization

The visual observation of the synthesis of *C. decidua* -mediated FeNPs was based on the typical chromatic change between the light yellow-green color of the fresh leaf extract, which turned dark brown and then black after the addition of a ferric chloride solution under heat conditions. This color change is one of the characteristics of synthesis of nanoparticles explained by surface plasmon resonance effects and d-d transitions of the iron oxide structure. The colloidal suspension also showed strong absorption peaks at 242, 385, 422 and 477 nm as revealed by UV-visible spectroscopic analysis (**Figure 1**). The absorption at 242 nm is due to

the use of $\pi \rightarrow \pi^*$ transitions of aromatic phytochemicals, and the observed 385 and 422 nm are explained by the fact that ligand to metal transfer (LMCT) transitions and crystal field transitions of d-d transitions of Fe^{3+} ions in octahedral coordination environments of the iron oxide structure (Behera et al., 2012). The wide absorption that spills to the visible range (477nm) also supports the existence of nanoscale-sized iron oxide nanoparticles which are in line with quantum confinement effects.

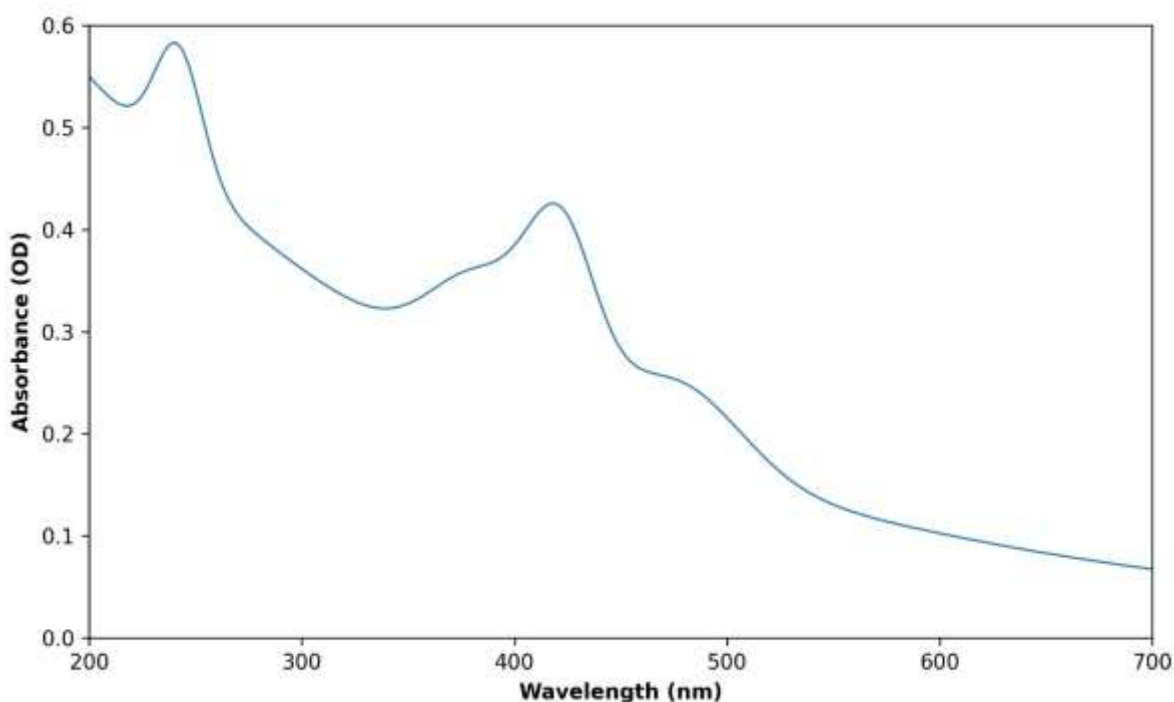


Figure1: UV-Vis spectrum of Capparis decidua derived FeNP's.

3.2 Functional Group Analysis via FTIR Spectroscopy.

FTIR spectroscopy gave important information as to the phytochemical constituents that are involved in bioreduction and stabilization of nanoparticles (**Figure 2**). There were strong absorption bands at 3403.24 and 3356.71 cm^{-1} , which is an OH stretch of phenolic hydroxyl and adsorbed water on the spectrum (Khan et al., 2018). These phenolic compounds are primary electron donors in the reduction of Fe^{3+} to lower oxidation states or oxide forms by the oxidation of hydroxyl groups to quinone structures (Amini & Akbari, 2019). Peaks in the absorption are at 2921.20 and 2837.03 cm^{-1} which are asymmetric and symmetric C-H stretches of aliphatic methylene groups found in fatty acids and terpenoids. Especially, it is

noteworthy that the absorption bands at 1643.00 and 1541.90 cm^{-1} , which are attributed to amide I (C=O stretch) and amide II (N-H bending), respectively, are of particular significance (Faghihzadeh et al., 2016). The presence of these amide functionalities is strong indicators of the presence of proteinaceous matter in the stabilization of nanoparticles by coordination between amino acid residues (histidine, cysteine, aspartate) and the iron oxide surface. The highest point of 1450.37 cm^{-1} represents aromatic C=C vibration of the chemical bonds, and 1189.54 and 1048.37 cm^{-1} are the bands of C-O vibration of glycosidic bond in polysaccharides and flavonoid glycosides. More importantly, the absorption band at 664.47 cm^{-1} corresponds with the typical Fe-O stretching vibration, which undoubtedly confirm the creation of iron oxide nanoparticles (Kumar et al., 2021). The FTIR analysis overall shows that the phytochemical corona consisting of polyphenols, proteins and polysaccharides is not lost after synthesis in the form of reductive ability during this process and long-term colloidal stabilization of the product by steric and electrostatic effects.

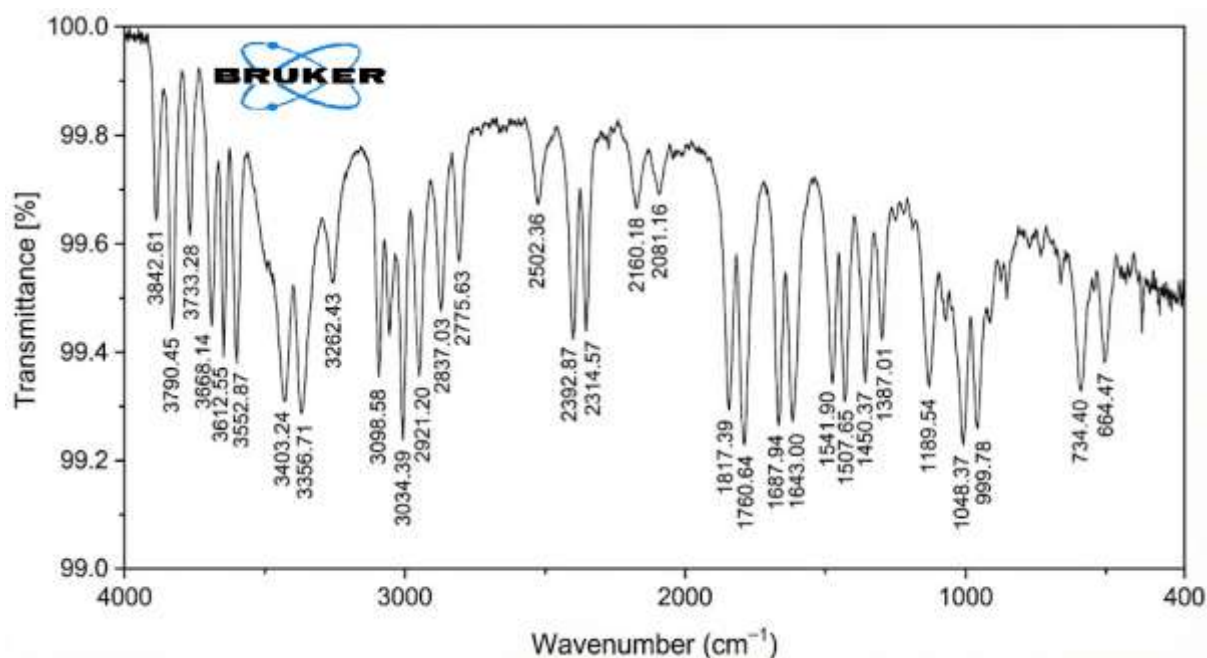


Figure 2: FTIR spectra of Capparis decidua derived FeNP's.

3.3 Morphological and Size Distribution Analysis

SEM analysis showed that FeNPs produced are mostly spherical with relatively homogeneous size distribution with minimal aggregation (**Figure 3A**). SEM micrographs were analyzed using dimensional analysis which revealed that the particles had a range of 48 to 87 nm with

most of the particles having a diameter of 65 nm. The thermodynamical advantage of the geometry is to minimize the surface energy and is associated with the isotropic growth conditions that are maintained when synthesizing them (Das et al., 2020). Measurements of dynamic light scattering produced an intensity-weighted mean hydrodynamic diameter (Z-average) of 88.5 nm, with the majority population at 76.33 nm (**Figure 3B**). The observed slightly bigger hydrodynamic diameter than the geometric core dimensions due to SEM is due to the hydrated phytochemical corona around the nanoparticle core, and to the solvation shell which adds to the effective hydrodynamic radius in aqueous dispersion. The polydispersity index (PDI) of 0.24 is evidence of a relatively small collection of sizes, indicating that one homogenous kinetic process occurred in the synthesis of the material.

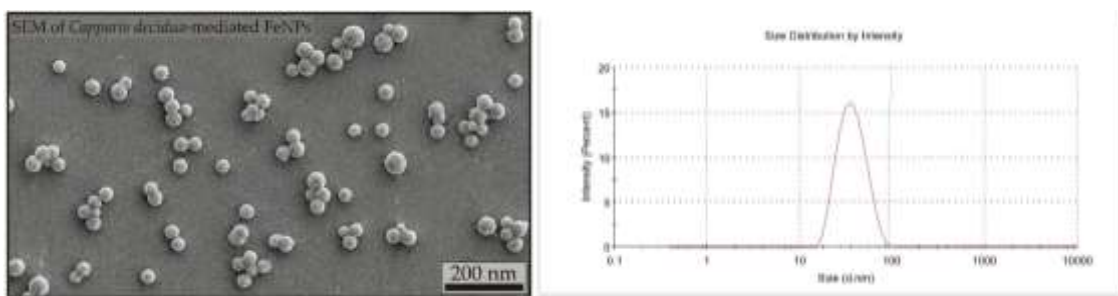


Figure 3: A) SEM, B) Zeta size of *Capparis decidua* derived FeNP's.

3.4 Colloidal Stability Assessment

Colloidal Stability Assessment is an evaluation that considers how the nanoparticles are dispersed in the solution, their size and shape, along with the characteristics of the surrounding water medium. The measured zeta potential of -28.3 mv revealed moderate and high colloidal stability of the FeNP suspension (**Figure 4**). Zeta potentials above ± 25 mV usually provide sufficient repulsive forces at the electrostatic level to prevent aggregation of the particles through electrical double-layers repulsion (Safer et al., 2019). The adsorbed phytochemicals are deprotonated to form a negative surface charge at the physiological pH, which forms an electrostatic barrier to coagulation. Moreover, the electrostatic stabilization mechanism is supplemented by steric stabilization of polymeric biomolecules including proteins and polysaccharides, which serve to provide long-term colloidal stability required by the biologic processes and storage. The strong colloidal stability of *C. decidua*-mediated

FeNPs means that no synthetic surfactants or stabilizing agents are required, which further supports the benefits of phytochemical-mediated synthesis.

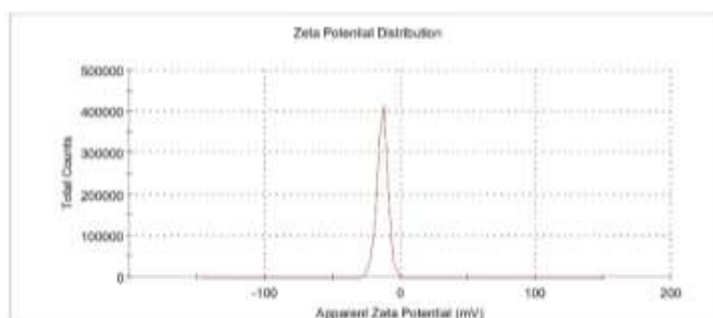


Figure 4: Zeta potential of Capparis decidua derived FeNP's.

3.5 Multifunctional Antioxidant Activity

The antioxidant activity of FeNPs mediated by *C. decidua* was thoroughly tested using three different complementary radical scavenging tests on different reactive species. **Table 1** shows the dose-dependent scavenging capacities in all three assays, which has shown an incremental formation of radical neutralization with increase in nanoparticle concentration.

Table 1. Concentration-dependent antioxidant activities of Capparis decidua-mediated FeNPs across complementary radical scavenging assays.

| Concentration (µg/mL) | DPPH Inhibition (%) | ABTS Inhibition (%) | NO Inhibition (%) |
|--------------------------------|---------------------|---------------------|---------------------|
| 20 | 15.05 ± 0.71 | 8.24 ± 1.33 | 17.00 ± 1.23 |
| 40 | 34.27 ± 2.43 | 24.00 ± 0.80 | 30.53 ± 2.76 |
| 60 | 51.00 ± 1.87 | 56.81 ± 1.57 | 43.82 ± 1.45 |
| 80 | 63.81 ± 0.56 | 64.57 ± 2.29 | 64.93 ± 0.52 |
| 100 | 74.44 ± 1.17 | 70.57 ± 1.38 | 80.05 ± 0.80 |
| IC₅₀ (µg/mL) | 47.82 ± 1.86 | 64.31 ± 0.97 | 68.54 ± 0.79 |

**Data presented as mean ± SD (n=3). DPPH: 1,1-diphenyl-2-picrylhydrazyl; ABTS: 2,2'-azino-bis(3-ethylbenzothiazoline-6-sulfonic acid); NO: nitric oxide; IC₅₀: half maximal inhibitory concentration.

3.5.1 DPPH Radical Scavenging Activity



The concentration-dependent scavenging ability was indicated by the DPPH assay, which measures the amount of hydrogen atoms or electrons donated to the stable DPPH radical. The DPPH scavenging activity was measured to be $15.05 \pm 0.71\%$ at $20 \mu\text{g/mL}$ to $74.44 \pm 1.17\%$ at $100 \mu\text{g/mL}$ (**Table 1**). The resulting IC_{50} of $47.82 \pm 1.86 \mu\text{g/mL}$ is comparable to a control standard of ascorbic acid, (IC_{50} : $43.25 \pm 1.15 \mu\text{g/mL}$) meaning that the FeNPs have antioxidant properties similar to a low-molecular-weight antioxidant. This higher DPPH scavenging activity is probably due to synergistic effects of the phytochemical corona, which is enriched in polyphenols with direct radical quenching ability by hydrogen atom transfer, as well as the iron oxide core, which might contribute catalytic breakdown of reactive species through redox cycling between the oxidation state of Fe^{2+} and Fe^{3+} .

3.5.2. The ABTS Radical Cation Scavenging activity was determined as follows:

The ABTS^+ assay assess antioxidant capacity by electron transfer, which compliments hydrogen atom transfer based-assays. The percentages of FeNPs scavenging ABTS were found to be rising between $8.24 \pm 1.33\%$ ($0.20 \mu\text{g/mL}$) and $70.57 \pm 1.38\%$ ($100 \mu\text{g/mL}$), with an IC_{50} of $64.31 \pm 0.97 \mu\text{g/mL}$ (**Table 1**). Even though this is marginally greater than the DPPH IC_{50} , it is indicative of strong antioxidant activity. The ABTS assay is performed in aqueous media and identifies both hydrophilic and lipophilic antioxidants and therefore the wide range of phytochemical constituents of the nanoparticle corona appears to work collaboratively to achieve the activity.

3.5.3 Nitric Oxide Radical Scavenging Activity

The activity of the nitric oxide radical scavenging was determined by the effective dissociation process between the test and the nitric oxide radical in the presence of HCl acid. Special clinical significance is attached to nitric oxide radical scavenging, whereby, overproduction of NO is a cause of inflammatory diseases, neurodegenerative diseases and cardiovascular diseases due to peroxynitrite and other reactive nitrogen species (Awah & Verla, 2010). The FeNPs exhibited superior NO scavenging ability with percentage inhibitions ranging $17.00 \pm 1.23\%$ to $80.05 \pm 0.80\%$ in the range of $20\text{-}100 \mu\text{g/mL}$ (**Table 1**). The IC_{50} of $68.54 \pm 0.79 \mu\text{g/mL}$ to is a significant therapeutic potential in the management of nitrosative stressful states, even though it is a bit greater than the control of ascorbic acid ($65.12 \mu\text{g/mL}$). The increased performance at high concentrations (80.05% at $100 \mu\text{g/mL}$)



indicates that the nanoparticles might have other mechanisms other than the mere radical scavenging, which might include the catalysis-decomposing processes via surface-exposed iron centers.

3.6 Attempts to understand Mechanistically the Antioxidant activity.

The synergistic antioxidant activity of the FeNPs mediated by *C.decidua* can be explained by a number of synergistic processes. The first is the phytochemical corona, which is rich in polyphenolic compounds (quercetin, catechin, gallic acid, and chlorogenic acid) that have inherent radical scavenging capacity through hydrogen atom donation, electron transfer and metallic chelation (Mohamad et al., 2014). Second, the iron oxide core can also play the role by Fenton-like reactions under redox-related conditions, catalysing the breakdown of active oxygen species. Third, nanoparticle architecture harbours multiple antioxidant moieties in confined spatial domains where there is a possibility of cooperativity effects where antioxidation of one moiety into adjacent antioxidants occurs through the electron delocalisation of the phytochemical network (Singh et al., 2023). Fourth, due to the dimensions imparted by nanochemistry, nanoscale size provides surface chemical accessibility and cellular penetration when compared to bulk materials or molecular antioxidants, enabling intracellular radical neutralisation. Comparative literature shows that *C.decidua*-mediated FeNPs have a better or equal antioxidant effect when compared to nanoparticles prepared by other plant extracts. As an example, iron oxide nanoparticles prepared with *Azadirachta indica* extracts showed DPPH IC₅₀ 55-72 µg/mL (Gautam et al., 2018; Salgado et al., 2019). The IC₅₀ value of 47.82 µg/ml of the present study puts *C. decidua*-mediated FeNPs in the category of the most effective phytochemical iron oxide nanoparticles.

3.7 Therapeutic Application Implications.

The combination of sustainable synthesis, strong physicochemical character, and strong multifunctional antioxidant activity makes *C.decidua*-FeNPs the prospective candidates in a variety of therapeutic strategies. Oxidative stress is a key pathogenic process in most chronic diseases, such as cancer, diabetes, cardiovascular diseases, and neurodegenerative diseases (Lee et al., 2011). The radical scavenging properties evident in the present case are exceptionally high, implying that it can be used as an adjunctive antioxidant therapy, or as an



ingredient in nutraceutical preparations. Additionally, intrinsic biocompatibility offered by phytochemical capping and magnetism hyperthermia feature of iron oxide nanoparticles allow the application of the latter in multifunctional mode, including targeted delivery of drugs, magnetic hyperthermia, and diagnostic imaging (Parveen et al., 2018). The negative zeta potential and colloidal stability allow subsequent surface functionalisation with targeting ligands, therapeutic payloads or diagnostic probes hence enabling the creation of theranostic nanoplatforms that combine diagnostic and therapeutic functionality.

4. Conclusion

This study illustrates the easy, inexpensive and eco-friendly green synthesis of iron oxide nanoparticles that were catalysed by *Capparis decidua* extract. The obtained nanoparticles were spherical, with a fine size distribution (48-87nm), strong colloidal stability ($\zeta = -28.3\text{mV}$), and high multifunctional antioxidant properties. Formation of nanoparticles was characterized through comprehensive physicochemical analysis involving UV-visible spectroscopy, FTIR, SEM and DLS which confirmed the formation of a phytochemical corona in the presence of polyphenols, proteins and polysaccharides that has a dual role in bioreduction and stabilization. The produced FeNPs have strong radical scavenging activities in complementary tests (DPPH IC_{50} : 47.82 $\mu\text{g/mL}$; ABTS IC_{50} : 64.31 $\mu\text{g/mL}$; NO IC_{50} : 68.54 $\mu\text{g/mL}$) comparable to the activities of conventional antioxidants, including ascorbic acid. These results endorse *C. decidua* as a useful botanical platform to prepare functional nanomaterials and place the following FeNPs at the centre stage of therapeutic interventions of oxidative stress-related diseases. Research directions in the future should include the systematic cytotoxicity tests on normal and cancerous cell lines to determine biocompatibility profiles and indices of therapy. Animal models Pharmacokinetic and biodistribution *in-vivo* studies should be performed to determine bioavailability, tissue retention and elimination routes. The study of antimicrobial effects with respect to clinically worthy pathogens, including multidrug-resistant strains, would expand the therapeutic application of these nanoparticles.

References

1. Amini, S. M., & Akbari, A. (2019). Metal nanoparticles synthesis through natural phenolic acids. *IET nanobiotechnology*, 13(8), 771-777.



2. Awah, F. M., & Verla, A. W. (2010). Antioxidant activity, nitric oxide scavenging activity and phenolic contents of *Ocimum gratissimum* leaf extract. *Journal of Medicinal Plants Research*, 4(24), 2479-2487.
3. Behera, S. S., Patra, J. K., Pramanik, K., Panda, N., & Thatoi, H. (2012). Characterization and evaluation of antibacterial activities of chemically synthesized iron oxide nanoparticles.
4. Chakraborty, N., Banerjee, J., Chakraborty, P., Banerjee, A., Chanda, S., Ray, K., ... & Sarkar, J. (2022). Green synthesis of copper/copper oxide nanoparticles and their applications: a review. *Green Chemistry Letters and Reviews*, 15(1), 187-215.
5. Das, S., Diyali, S., Vinothini, G., Perumalsamy, B., Balakrishnan, G., Ramasamy, T., ... & Biswas, B. (2020). Synthesis, morphological analysis, antibacterial activity of iron oxide nanoparticles and the cytotoxic effect on lung cancer cell line. *Heliyon*, 6(9).
6. Faghihzadeh, F., Anaya, N. M., Schifman, L. A., & Oyanedel-Craver, V. (2016). Fourier transform infrared spectroscopy to assess molecular-level changes in microorganisms exposed to nanoparticles. *Nanotechnology for Environmental Engineering*, 1(1), 1.
7. Gautam, A., Rawat, S., Verma, L., Singh, J., Sikarwar, S., Yadav, B. C., & Kalamdhad, A. S. (2018). Green synthesis of iron nanoparticle from extract of waste tea: An application for phenol red removal from aqueous solution. *Environmental nanotechnology, monitoring & management*, 10, 377-387.
8. Khan, S. A., Khan, S. B., Khan, L. U., Farooq, A., Akhtar, K., & Asiri, A. M. (2018). Fourier transform infrared spectroscopy: fundamentals and application in functional groups and nanomaterials characterization. In *Handbook of materials characterization* (pp. 317-344). Cham: Springer International Publishing.
9. Kumar, S., Kumar, M., & Singh, A. (2021). Synthesis and characterization of iron oxide nanoparticles (Fe₂O₃, Fe₃O₄): a brief review. *Contemporary Physics*, 62(3), 144-164.
10. Lee, J., Kim, H. Y., Zhou, H., Hwang, S., Koh, K., Han, D. W., & Lee, J. (2011). Green synthesis of phytochemical-stabilized Au nanoparticles under ambient conditions and their biocompatibility and antioxidative activity. *Journal of Materials Chemistry*, 21(35), 13316-13326.
11. Mohamad, N. A. N., Arham, N. A., Jai, J., & Hadi, A. (2014). Plant extract as reducing agent in synthesis of metallic nanoparticles: a review. *Advanced Materials Research*, 832, 350-355.



12. Ovais, M., Khalil, A. T., Islam, N. U., Ahmad, I., Ayaz, M., Saravanan, M., ... & Mukherjee, S. (2018). Role of plant phytochemicals and microbial enzymes in biosynthesis of metallic nanoparticles. *Applied microbiology and biotechnology*, 102(16), 6799-6814.
13. Parveen, S., Wani, A. H., Shah, M. A., Devi, H. S., Bhat, M. Y., & Koka, J. A. (2018). Preparation, characterization and antifungal activity of iron oxide nanoparticles. *Microbial pathogenesis*, 115, 287-292.
14. Pradeep, M., Kruszka, D., Kachlicki, P., Mondal, D., & Franklin, G. (2021). Uncovering the phytochemical basis and the mechanism of plant extract-mediated eco-friendly synthesis of silver nanoparticles using ultra-performance liquid chromatography coupled with a photodiode array and high-resolution mass spectrometry. *ACS Sustainable Chemistry & Engineering*, 10(1), 562-571.
15. Safer, A. M., Leporatti, S., Jose, J., & Soliman, M. S. (2019). Conjugation of EGCG and chitosan NPs as a novel nano-drug delivery system. *International Journal of Nanomedicine*, 8033-8046.
16. Salgado, P., Márquez, K., Rubilar, O., Contreras, D., & Vidal, G. (2019). The effect of phenolic compounds on the green synthesis of iron nanoparticles (FexOy-NPs) with photocatalytic activity. *Applied Nanoscience*, 9(3), 371-385.
17. Shaikh, W. A., Chakraborty, S., Owens, G., & Islam, R. U. (2021). A review of the phytochemical mediated synthesis of AgNP (silver nanoparticle): The wonder particle of the past decade. *Applied Nanoscience*, 11(11), 2625-2660.
18. Singh, H., Desimone, M. F., Pandya, S., Jasani, S., George, N., Adnan, M., ... & Alderhami, S. A. (2023). Revisiting the green synthesis of nanoparticles: uncovering influences of plant extracts as reducing agents for enhanced synthesis efficiency and its biomedical applications. *International journal of nanomedicine*, 4727-4750.
19. Singh, P., Mishra, G., Srivastava, S., Jha, K. K., & Khosa, R. L. (2011). Traditional uses, phytochemistry and pharmacological properties of Capparis decidua: An overview. *Der Pharmacia Lettre*, 3(2), 71-82.